



HAL
open science

DDFV Schemes for semiconductors energy-transport models

Giulia Lissoni

► **To cite this version:**

Giulia Lissoni. DDFV Schemes for semiconductors energy-transport models. ALGORITMY 2020 - Conference on Scientific Computing, Sep 2020, Podbanske, Slovakia. hal-02899787

HAL Id: hal-02899787

<https://hal.science/hal-02899787>

Submitted on 15 Jul 2020

HAL is a multi-disciplinary open access archive for the deposit and dissemination of scientific research documents, whether they are published or not. The documents may come from teaching and research institutions in France or abroad, or from public or private research centers.

L'archive ouverte pluridisciplinaire **HAL**, est destinée au dépôt et à la diffusion de documents scientifiques de niveau recherche, publiés ou non, émanant des établissements d'enseignement et de recherche français ou étrangers, des laboratoires publics ou privés.

DDFV SCHEMES FOR SEMICONDUCTORS ENERGY-TRANSPORT MODELS*

GIULIA LISSONI†

Abstract. We propose a Discrete Duality Finite Volume scheme (DDFV for short) for an energy transport model for semiconductors. As in the continuous case, thanks to a change of variables into the so-called "entropic variables", we are able to prove a discrete entropy-dissipation estimate, which gives *a priori* estimates for the problem. We perform some numerical tests for the 2D ballistic diode, by comparing the Chen model and the Lyumkis model.

Key words. DDFV, finite volumes, energy-transport, semiconductor device, diode.

AMS subject classifications. 65M08, 65M12, 35Q81

1. Introduction. In the modelling of semiconductor devices, we can distinguish between kinetic models and fluid dynamical models (see for instance [11]). Energy-transport models belong to the class of fluid dynamical models; they describe the flow of electrons through a semiconductor crystal, which is influenced by diffusive, electrical and thermal effects. They are coupled systems of parabolic and elliptic equations, which are well suited for numerical simulations by finite volume methods. These equations can be re-written in a drift-diffusion form, which can be interesting for the numerical simulations; we can cite the works of [8, 6, 10] for the stationary systems, [3, 4] for the evolutive case. However, up to our knowledge, there exists no convergence analysis of these numerical schemes; a first work in this direction is the work of [2], in the context of finite volume schemes with two-point flux approximations. They reproduce at the discrete level the analysis done in [5], where the authors prove the existence of a weak solution for the energy transport model in its original formulation; it is possible through a transformation of the problem by means of *entropic variables*, which symmetrize the problem and allow to prove *a priori* estimates by using an entropy function. Our goal is to extend the work done in [2] to the case of general meshes.

In order to do so, our choice is to discretize the model described in [5] with Discrete Duality Finite Volume ("DDFV" for short) schemes; their introduction dates back to [9, 7], for the study of the Laplace equation on a large class of 2D meshes including non-conformal and distorted meshes. Such schemes require unknowns on both vertices and centers of primal control volumes. This leads to reconstruct two-dimensional discrete gradient and divergence operators which are in duality in a discrete sense. This kind of construction has two main advantages: it allows to consider general meshes (that do not necessarily verify the classical orthogonality condition required by finite volume meshes) and to reconstruct and mimic at the discrete level the dual properties of the continuous differential operators.

Outline. This paper is organized as follows. In Sec. 2, we present the model. In Sec. 3, we first recall the DDFV framework, then we introduce the DDFV schemes corresponding to the model described in Sec. 2 and we state some properties of these schemes. Finally, in Sec. 4, we discuss some numerical results for the 2D ballistic diode.

2. The model. The energy transport system consists in two continuity equations for the electron density ρ_1 and the internal energy density ρ_2 coupled with a Poisson equation for the

*This work was supported by ANR MoHyCon (ANR-17-CE40-0027-01).

†Université de Nantes, LMJL, CNRS (giulia.lissoni@univ-nantes.fr).

electrical potential V . Let $\Omega \subset \mathbb{R}^2$ be an open bounded polygonal with $\partial\Omega = \Gamma_D \cup \Gamma_N$, $\Gamma_D \cup \Gamma_N = \emptyset$ and $m(\Gamma_D) > 0$ and let $t^* > 0$. Let μ be the chemical potential and T the temperature of the lattice; the unknowns of the problem are $\mathbf{u} = (u_1, u_2)$, $u_i(t, \mathbf{x}) : [0, t^*] \times \Omega \rightarrow \mathbb{R}$, $i = 1, 2$, defined by: $u_1 = \mu/T$, $u_2 = -1/T$, and the electrostatic potential $V(t, \mathbf{x}) : [0, t^*] \times \Omega \rightarrow \mathbb{R}$; ρ_1, ρ_2 are given functions of \mathbf{u} . The energy transport model writes:

$$\begin{cases} \partial_t \rho_1(\mathbf{u}) + \operatorname{div}(J_1(\mathbf{u})) = 0 & \text{in } [0, t^*] \times \Omega, \\ \partial_t \rho_2(\mathbf{u}) + \operatorname{div}(J_2(\mathbf{u})) = \nabla V \cdot J_1(\mathbf{u}) + W(\mathbf{u}) & \text{in } [0, t^*] \times \Omega, \\ -\lambda^2 \Delta V = C(\mathbf{x}) - \rho_1(\mathbf{u}) & \text{in } [0, t^*] \times \Omega, \end{cases} \quad (2.1)$$

where J_1 is the current density of electrons, J_2 is the current density of energy, $W(\mathbf{u})$ is the energy relaxation term, $\nabla V \cdot J_1$ is the Joule heating term, $C(\mathbf{x})$ is the initial doping profile and λ is the rescaled Debye length. The current densities are defined by:

$$J_i(\mathbf{u}) = -L_{i1}(\nabla u_1 + u_2 \nabla V) - L_{i2} \nabla u_2 \in \mathbb{R}^2, \quad \text{for } i = 1, 2. \quad (2.2)$$

The quantities L_{ij} actually depend on \mathbf{u} and may be written as coefficients of a symmetric uniformly positive definite matrix $L = (L_{ij})$.

The system is coupled with mixed Dirichlet/Neumann boundary conditions and an initial data:

$$\begin{cases} u_1(t, \mathbf{x}) = g_1(\mathbf{x}), u_2(t, \mathbf{x}) = g_2(\mathbf{x}), V(t, \mathbf{x}) = h(\mathbf{x}) & \text{on } [0, t^*] \times \Gamma_D, \\ J_1 \cdot \bar{\mathbf{n}} = J_2 \cdot \bar{\mathbf{n}} = \nabla V \cdot \bar{\mathbf{n}} = 0 & \text{on } [0, t^*] \times \Gamma_N, \\ u_1(0, \mathbf{x}) = u_{1,init}(\mathbf{x}), u_2(0, \mathbf{x}) = u_{2,init}(\mathbf{x}) & \text{in } \Omega, \end{cases} \quad (2.3)$$

where Γ_D denotes the Ohmic contacts and Γ_N the insulating segments.

HYP 2.1 (Model assumptions.). *We suppose that:*

1. *The function $\rho = (\rho_1, \rho_2)$ is strongly monotone in the sense that there exists a constant C_0 such that*

$$(\rho(\mathbf{u}) - \rho(\mathbf{v})) \cdot (\mathbf{u} - \mathbf{v}) \geq C_0 |\mathbf{u} - \mathbf{v}|^2, \quad \mathbf{u}, \mathbf{v} \in \mathbb{R}^2.$$

We assume that ρ derives from a potential, that is $\exists \chi \in C^1$ strictly convex such that $\rho = \nabla \chi$.

2. *The matrix L is symmetric, uniformly positive definite.*
3. *The Dirichlet boundary conditions g_1, g_2, h do not depend on time and are traces of some functions defined on the whole domain Ω , still denoted by g_1, g_2, h . Moreover, we assume that $g_2 < 0$ is constant on Γ_D .*
4. *The energy relaxation term W is such that for all $\mathbf{u} \in \mathbb{R}^2$ and $g_2 < 0$: $W(\mathbf{u})(u_2 - g_2) \leq 0$.*

Under the assumptions of Hyp. 2.1, in [5], existence of solutions of the stationary and transient model (2.1)-(2.3) is proved thanks to a reformulation of the system in terms of dual entropic variables, which symmetrizes the equations and allows to derive an entropy-dissipation estimate. Our goal is to adopt this framework and to reproduce it at a discrete level. In the following section, we introduce the system reformulated in terms of entropic variables and the entropy structure.

2.1. The system in entropic variables. The key point of the analysis of the primal model (2.1)-(2.3) is to use another set of variables which symmetrizes the problem, see [5]. We define the so-called *entropic variables* (or *electrochemical potentials*) $\mathbf{w} = (w_1, w_2)$:

$$\begin{cases} w_1 = u_1 + u_2 V, \\ w_2 = u_2. \end{cases} \quad (2.4)$$

Then (2.1)-(2.3) is equivalent to:

$$\begin{cases} \partial_t b_1(\mathbf{w}, V) + \operatorname{div}(I_1(\mathbf{w}, V)) = 0 & \text{in } [0, t^*] \times \Omega, \\ \partial_t b_2(\mathbf{w}, V) + \operatorname{div}(I_2(\mathbf{w}, V)) = -\partial_t V b_1(\mathbf{w}, V) + \bar{W}(\mathbf{w}, V) & \text{in } [0, t^*] \times \Omega, \\ -\lambda^2 \Delta V = C(\mathbf{x}) - b_1(\mathbf{w}, V) & \text{in } [0, t^*] \times \Omega, \end{cases} \quad (2.5)$$

coupled with

$$\begin{cases} w_1(t, \mathbf{x}) = \bar{g}_1(\mathbf{x}), w_2(t, \mathbf{x}) = \bar{g}_2(\mathbf{x}), V(t, \mathbf{x}) = \bar{g}(\mathbf{x}) & \text{on } [0, t^*] \times \Gamma_D, \\ I_1 \cdot \bar{\mathbf{n}} = I_2 \cdot \bar{\mathbf{n}} = \nabla V \cdot \bar{\mathbf{n}} = 0 & \text{on } [0, t^*] \times \Gamma_N, \\ w_1(0, \mathbf{x}) = w_{1,init}(\mathbf{x}), w_2(0, \mathbf{x}) = w_{2,init}(\mathbf{x}) & \text{in } \Omega, \end{cases} \quad (2.6)$$

where

$$\begin{cases} b_1(\mathbf{w}, V) = \rho_1(\mathbf{u}), \\ b_2(\mathbf{w}, V) = \rho_2(\mathbf{u}) - V \rho_1(\mathbf{u}), \end{cases}$$

and

$$I_i(\mathbf{u}) = -D_{i1} \nabla w_1 - D_{i2} \nabla w_2 \in \mathbb{R}^2, \quad \text{for } i = 1, 2.$$

The diffusion coefficients form the symmetric matrix $D = (D_{ij})$, defined by:

$$D = {}^t P L P \text{ with } P = \begin{pmatrix} 1 & -V \\ 0 & 1 \end{pmatrix}, \quad (2.7)$$

so the new diffusion matrix D is also symmetric and positive definite.

2.2. Entropy structure. In [5], existence results for the model (2.1)-(2.3) are based on entropy estimates, which are obtained thanks to the reformulation in entropic variables. The *entropy function* is defined by:

$$S(t) = \int_{\Omega} [\rho(\mathbf{u}) \cdot (\mathbf{u} - \mathbf{g}) - (\chi(\mathbf{u}) - \chi(\mathbf{g}))] dx - \frac{\lambda^2}{2} g_2 \int_{\Omega} |\nabla(V - h)|^2 dx, \quad (2.8)$$

where $\mathbf{g} = (g_1, g_2)$ and h are the Dirichlet data. Since, by Hyp. 2.1, $g_2 < 0$, and χ is a convex function such that $\rho = \nabla \chi$, $S(t)$ is nonnegative for all $t \geq 0$.

PROPOSITION 2.2. *Assuming that Hyp. 2.1 is verified and that the Dirichlet boundary conditions are in thermal equilibrium, i.e. $\nabla \bar{g}_1 = \nabla \bar{g}_2 = 0$, the entropy function satisfies:*

$$\frac{d}{dt} S(t) = - \int_{\Omega} {}^t \nabla w D \nabla w + \int_{\Omega} W(u_2 - g_2) \leq 0.$$

3. DDFV discretization.

3.1. DDFV framework. Here and below, we adopt the definitions and notations introduced in [1, 13]; for more details, see the references.

Meshes. DDFV method requires unknowns on vertices, centers and edges of control volumes; for this reason, it works on (three) staggered meshes. From an initial mesh, called the "primal mesh" (denoted with $\mathfrak{M} \cup \partial \mathfrak{M}$), we construct the "dual mesh" (denoted with $\mathfrak{M}^* \cup \partial \mathfrak{M}^*$), that is centered on the vertices of the primal mesh, and the "diamond mesh" (denoted with \mathfrak{D}), which is

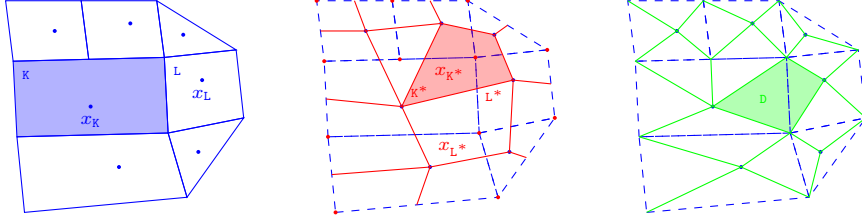


Fig. 3.1: DDFV meshes on a non conformal mesh: primal mesh $\mathfrak{M} \cup \partial\mathfrak{M}$ (blue), dual mesh $\mathfrak{M}^* \cup \partial\mathfrak{M}^*$ (red) and diamond mesh \mathfrak{D} (green).

centered on the edges of the primal mesh; see Fig. 3.1 for an illustration. The union of primal and dual meshes will be denoted by \mathfrak{T} .

We consider a primal mesh \mathfrak{M} consisting of open disjoint polygons κ called primal cells, such that $\bigcup_{\kappa \in \mathfrak{M}} \bar{\kappa} = \bar{\Omega}$. We denote $\partial\mathfrak{M}$ the set of edges of the primal mesh included in $\partial\Omega$, that are considered as degenerated primal cells. We associate to each κ a point x_κ , called center, and we denote by m_κ its measure. For the volumes of the boundary, the point x_κ is situated at the mid point of the edge. When κ and L are neighboring volumes, we suppose that $\partial\kappa \cap \partial L$ is a segment denoted by $\sigma = \kappa|L$, edge of the primal mesh \mathfrak{M} . Let \mathcal{E} be the set of all edges and $\mathcal{E}_{int} = \mathcal{E} \setminus \{\sigma \in \mathcal{E} \text{ such that } \sigma \subset \partial\Omega\}$. The DDFV framework is free of further "admissibility constraint", in particular we do not need to assume the orthogonality of the segment x_κ, x_L with $\sigma = \kappa|L$.

From this primal mesh, we build the associated dual mesh. A dual cell κ^* is associated to a vertex x_{κ^*} of the primal mesh. The dual cells are obtained by joining the centers of the primal control volumes that have x_{κ^*} as vertex. Then, the point x_{κ^*} is called center of κ^* and we denote by m_{κ^*} its measure. We will distinguish interior dual mesh, for which x_{κ^*} does not belong to $\partial\Omega$, denoted by \mathfrak{M}^* and the boundary dual mesh, for which x_{κ^*} belongs to $\partial\Omega$, denoted by $\partial\mathfrak{M}^*$. We denote with $\sigma^* = \kappa^*|L^*$ the edges of the dual mesh $\mathfrak{M}^* \cup \partial\mathfrak{M}^*$ and \mathcal{E}^* the set of these edges.

The diamond mesh is made of quadrilaterals with disjoint interiors, such that their principal diagonals are a primal edge $\sigma = \kappa|L = [x_{\kappa^*}, x_{L^*}]$ and the dual edge $\sigma^* = [x_\kappa, x_L]$. These quadrilaterals are called diamonds and they are denoted with \mathfrak{D} or $\mathfrak{D}_{\sigma, \sigma^*}$. Thus a diamond is a quadrilateral with vertices $x_\kappa, x_L, x_{\kappa^*}$ and x_{L^*} . The set of all diamonds is denoted with \mathfrak{D} and we have $\Omega = \bigcup_{\mathfrak{D} \in \mathfrak{D}} \mathfrak{D}$. We distinguish the diamonds of the boundary and on the interior: $\mathfrak{D}_{ext} = \{\mathfrak{D}_{\sigma, \sigma^*} \in \mathfrak{D}, \text{ such that } \sigma \subset \partial\Omega\}$ and $\mathfrak{D}_{int} = \mathfrak{D} \setminus \mathfrak{D}_{ext}$. For a diamond cell \mathfrak{D} we note by $m_{\mathfrak{D}}$ its measure, m_σ the length of the primal edge σ , m_{σ^*} the length of the dual edge σ^* , \vec{n}_{σ^*} the unit vector normal to σ^* oriented from x_{κ^*} to x_{L^*} , \vec{n}_{σ} the unit vector normal to σ oriented from x_κ to x_L (see Fig. 3.2).

Unknowns. We associate to each primal volume $\kappa \in \mathfrak{M} \cup \partial\mathfrak{M}$ unknowns $\mathbf{u}_\kappa \in \mathbb{R}^2, V_\kappa \in \mathbb{R}$, and to every dual volume $\kappa^* \in \mathfrak{M}^* \cup \partial\mathfrak{M}^*$ unknowns $\mathbf{u}_{\kappa^*} \in \mathbb{R}^2, V_{\kappa^*} \in \mathbb{R}$. These unknowns are collected in the families:

$$\begin{aligned} \mathbf{u}_{\mathfrak{T}} &= ((\mathbf{u}_\kappa)_{\kappa \in (\mathfrak{M} \cup \partial\mathfrak{M})}, (\mathbf{u}_{\kappa^*})_{\kappa^* \in (\mathfrak{M}^* \cup \partial\mathfrak{M}^*)}) \in (\mathbb{R}^2)^{\mathfrak{T}}, \\ V_{\mathfrak{T}} &= ((V_\kappa)_{\kappa \in (\mathfrak{M} \cup \partial\mathfrak{M})}, (V_{\kappa^*})_{\kappa^* \in (\mathfrak{M}^* \cup \partial\mathfrak{M}^*)}) \in \mathbb{R}^{\mathfrak{T}}. \end{aligned}$$

Since we are considering mixed boundary conditions, we have to define two subspaces of the boundary meshes:

$$\begin{aligned} \partial\mathfrak{M}_D &= \{\kappa \in \partial\mathfrak{M} : x_\kappa \in \Gamma_D\}; & \partial\mathfrak{M}_N &= \{\kappa \in \partial\mathfrak{M} : x_\kappa \in \Gamma_N\}; \\ \partial\mathfrak{M}_D^* &= \{\kappa^* \in \partial\mathfrak{M}^* : x_{\kappa^*} \in \Gamma_D\}; & \partial\mathfrak{M}_N^* &= \{\kappa^* \in \partial\mathfrak{M}^* : x_{\kappa^*} \in \Gamma_N \setminus \Gamma_D\}; \end{aligned}$$

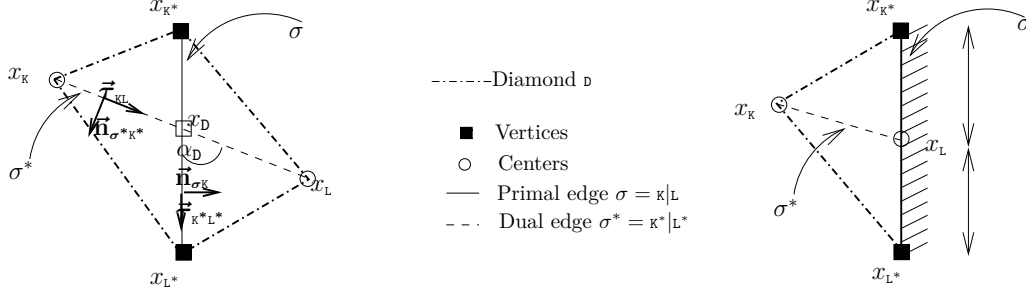


Fig. 3.2: A diamond $d = d_{\sigma, \sigma^*}$, on the interior (left) and on the boundary (right).

and the subspace of $(\mathbb{R}^d)^\mathfrak{I}$, $d = 1, 2$, useful to take into account Dirichlet boundary conditions:

$$\mathbb{E}_{m, \mathbf{g}}^{\Gamma_D} = \{\Phi_{\mathfrak{I}} \in (\mathbb{R}^d)^\mathfrak{I}, \text{ s. t. } \forall k \in \partial\mathfrak{M}_D, \Phi_k = (\mathbb{P}_m^\mathfrak{I} \mathbf{g})_k \text{ and } \forall k^* \in \partial\mathfrak{M}_D^*, \Phi_{k^*} = (\mathbb{P}_m^\mathfrak{I} \mathbf{g})_{k^*}\},$$

where $\mathbb{P}_m^\mathfrak{I}$ is a discrete average projection on the mesh.

Discrete operators. We define a piecewise constant approximation of the gradient operator of a vector of $\mathbb{R}^\mathfrak{I}$ as the operator $\nabla^{\mathfrak{D}} : \mathbf{u}_{\mathfrak{I}} \in \mathbb{R}^\mathfrak{I} \mapsto (\nabla^{\mathfrak{D}} \mathbf{u}_{\mathfrak{I}})_{\mathfrak{D} \in \mathfrak{D}} \in (\mathbb{R}^2)^\mathfrak{D}$, such that for $\mathfrak{D} \in \mathfrak{D}$:

$$\nabla^{\mathfrak{D}} \mathbf{u}_{\mathfrak{I}} = \frac{1}{\sin(\alpha_{\mathfrak{D}})} \left[\frac{u_L - u_k}{m_{\sigma^*}} \bar{\mathbf{n}}_{\sigma_k} + \frac{u_{L^*} - u_{k^*}}{m_{\sigma}} \bar{\mathbf{n}}_{\sigma^*_{k^*}} \right].$$

Its discrete dual operator is the approximation of the divergence operator of a vector of $(\mathbb{R}^2)^\mathfrak{D}$ denoted by $\text{div}^\mathfrak{I} : \xi_{\mathfrak{D}} \in (\mathbb{R}^2)^\mathfrak{D} \mapsto \text{div}^\mathfrak{I} \xi_{\mathfrak{D}} \in \mathbb{R}^\mathfrak{I}$, such that:

$$\begin{aligned} \text{div}^k \xi_{\mathfrak{D}} &= \frac{1}{m_k} \sum_{\mathfrak{D}_{\sigma, \sigma^*} \in \mathfrak{D}_k} m_{\sigma} \xi_{\mathfrak{D}} \cdot \bar{\mathbf{n}}_{\sigma_k}, \quad \forall k \in \mathfrak{M} \\ \text{div}^{k^*} \xi_{\mathfrak{D}} &= \frac{1}{m_{k^*}} \sum_{\mathfrak{D}_{\sigma, \sigma^*} \in \mathfrak{D}_{k^*}} m_{\sigma^*} \xi_{\mathfrak{D}} \cdot \bar{\mathbf{n}}_{\sigma^*_{k^*}}, \quad \forall k^* \in \mathfrak{M}^* \\ \text{div}^{k^*} \xi_{\mathfrak{D}} &= \frac{1}{m_{k^*}} \left(\sum_{\mathfrak{D}_{\sigma, \sigma^*} \in \mathfrak{D}_{k^*}} m_{\sigma^*} \xi_{\mathfrak{D}} \cdot \bar{\mathbf{n}}_{\sigma^*_{k^*}} + \sum_{\mathfrak{D}_{\sigma, \sigma^*} \in \mathfrak{D}_{k^*} \cap \mathfrak{D}_{ext}} \frac{m_{\sigma}}{2} \xi_{\mathfrak{D}} \cdot \bar{\mathbf{n}}_{\sigma_k} \right) \quad \forall k^* \in \partial\mathfrak{M}_N^*. \end{aligned}$$

The discrete gradient and the discrete divergence are in duality (which gives the name to the method), meaning that they are linked by a discrete Green's formula; see [1, 7, 13] for details.

Scalar products and norms. We define the scalar products on the approximation spaces, for $d = 1, 2$, as:

$$\begin{aligned} [[\mathbf{v}_{\mathfrak{I}}, \mathbf{u}_{\mathfrak{I}}]]_{\mathfrak{I}} &= \frac{1}{2} \left(\sum_{k \in \mathfrak{M}} m_k \mathbf{u}_k \cdot \mathbf{v}_k + \sum_{k^* \in \mathfrak{M}^* \cup \partial\mathfrak{M}_N^*} m_{k^*} \mathbf{u}_{k^*} \cdot \mathbf{v}_{k^*} \right) & \forall \mathbf{u}_{\mathfrak{I}}, \mathbf{v}_{\mathfrak{I}} \in (\mathbb{R}^d)^\mathfrak{I}, \\ (\Phi_{\mathfrak{D}}, \mathbf{v}_{\partial\mathfrak{M}})_{\partial\Omega} &= \sum_{\mathfrak{D}_{\sigma, \sigma^*} \in \mathfrak{D}_{ext}} m_{\sigma} \Phi_{\mathfrak{D}} \cdot \mathbf{v}_{\sigma} & \forall \Phi_{\mathfrak{D}} \in (\mathbb{R}^d)^\mathfrak{D}_{ext}, \mathbf{v}_{\partial\mathfrak{M}} \in (\mathbb{R}^d)^{\partial\mathfrak{M}}, \\ (\xi_{\mathfrak{D}}, \Phi_{\mathfrak{D}})_{\mathfrak{D}} &= \sum_{\mathfrak{D}_{\sigma, \sigma^*} \in \mathfrak{D}} m_{\sigma} \xi_{\mathfrak{D}} \cdot \Phi_{\mathfrak{D}} & \forall \xi_{\mathfrak{D}}, \Phi_{\mathfrak{D}} \in (\mathbb{R}^d)^\mathfrak{D}, \end{aligned}$$

to which we can associate norms, e.g. $\|\mathbf{u}_{\mathfrak{T}}\|_2 = [[\mathbf{u}_{\mathfrak{T}}, \mathbf{u}_{\mathfrak{T}}]]_{\mathfrak{T}}^{\frac{1}{2}}$, $\|\mathbf{p}_{\mathfrak{D}}\|_2 = (\mathbf{p}_{\mathfrak{D}}, \mathbf{p}_{\mathfrak{D}})_{\mathfrak{D}}^{\frac{1}{2}}$.

We also need to define a "**reconstruction**" operator $\gamma^{\mathfrak{D}} : \Phi_{\mathfrak{T}} \in \mathbb{R}^{\mathfrak{T}} \mapsto \gamma^{\mathfrak{D}}(\Phi_{\mathfrak{T}}) = (\gamma^{\mathfrak{D}}(\Phi_{\mathfrak{T}}))_{\mathfrak{D} \in \mathfrak{D}} \in \mathbb{R}^{\mathfrak{D}}$, in order to pass from \mathfrak{T} to \mathfrak{D} .

$$\begin{aligned} \gamma^{\mathfrak{D}}(\Phi_{\mathfrak{T}}) &= \frac{m_{\mathfrak{D} \cap \mathfrak{K}} \Phi_{\mathfrak{K}} + m_{\mathfrak{D} \cap \mathfrak{L}} \Phi_{\mathfrak{L}} + m_{\mathfrak{D} \cap \mathfrak{K}^*} \Phi_{\mathfrak{K}^*} + m_{\mathfrak{D} \cap \mathfrak{L}^*} \Phi_{\mathfrak{L}^*}}{2m_{\mathfrak{D}}} & \forall \mathfrak{D} \in \mathfrak{D} \setminus \mathfrak{D}_{ext}, \\ \gamma^{\mathfrak{D}}(\Phi_{\mathfrak{T}}) &= \frac{m_{\mathfrak{D} \cap \mathfrak{K}} \Phi_{\mathfrak{K}} + m_{\mathfrak{D} \cap \mathfrak{K}^*} \Phi_{\mathfrak{K}^*} + m_{\mathfrak{D} \cap \mathfrak{L}^*} \Phi_{\mathfrak{L}^*}}{2m_{\mathfrak{D}}} & \forall \mathfrak{D} \in \mathfrak{D}_{ext}. \end{aligned} \quad (3.1)$$

3.2. DDFV scheme for the energy-transport model. To obtain our scheme for (2.1)-(2.3), we integrate the equations over all $\mathfrak{M} \cup \mathfrak{M}^* \cup \partial\mathfrak{M}_N^*$. We impose strong Dirichlet boundary conditions on $\partial\mathfrak{M}_D \cup \partial\mathfrak{M}_D^*$ and Neumann boundary conditions on $\partial\mathfrak{M}_N$. To discretize the Joule heating term, as in [2], we rewrite it as:

$$\nabla V \cdot J_1(\mathbf{u}) = \operatorname{div}(V J_1(\mathbf{u})) - V \operatorname{div}(J_1(\mathbf{u})).$$

Let $N \in \mathbb{N}^*$. We note $\delta t = t^*/N$ and $t_n = n\delta t$ for $n \in \{0, \dots, N\}$. We choose to use an implicit Euler time discretization to avoid a constraining parabolic stability condition.

We look for $\mathbf{u}_{\mathfrak{T}}^{[0, t^*]} = (\mathbf{u}^n)_{n \in \{0, \dots, N\}} \in (\mathbb{E}_{\mathbf{g}}^{\Gamma_D})^{N+1}$ and $\mathbf{V}_{\mathfrak{T}}^{[0, t^*]} = (\mathbf{V}^n)_{n \in \{0, \dots, N\}} \in (\mathbb{E}_h^{\Gamma_D})^{N+1}$, that we initialize with:

$$\mathbf{u}^0 = \mathbb{P}_c^{\mathfrak{T}} \mathbf{u}_{init} \in \mathbb{E}_{\mathbf{g}}^{\Gamma_D}, \quad \mathbf{V}^0 = \mathbb{P}_c^{\mathfrak{T}} \mathbf{V}_{init} \in \mathbb{E}_h^{\Gamma_D},$$

where $\mathbb{P}_c^{\mathfrak{T}}$ is a centered projection on the mesh \mathfrak{T} .

REMARK 3.1. *The unknowns $(\mathbf{u}_{\mathfrak{T}}, \mathbf{V}_{\mathfrak{T}})$ are associated to the mesh \mathfrak{T} ; in order to discretize our system, it is sometimes necessary to reconstruct their values on the diamond mesh \mathfrak{D} . This is done by the operator (3.1); to simplify the notations, we will denote by $(\mathbf{u}_{\mathfrak{D}}, \mathbf{V}_{\mathfrak{D}})$ the reconstructions $(\gamma^{\mathfrak{D}}(\mathbf{u}_{\mathfrak{T}}), \gamma^{\mathfrak{D}}(\mathbf{V}_{\mathfrak{T}}))$.*

Thus, problem (2.1)-(2.3) is discretized as:

$$\left\{ \begin{array}{ll} \frac{\rho_{1,\mathfrak{K}}^{n+1} - \rho_{1,\mathfrak{K}}^n}{\delta t} + \operatorname{div}^{\mathfrak{K}}(J_{1,\mathfrak{D}}^{n+1}) = 0 & \forall \mathfrak{K} \in \mathfrak{M} \\ \frac{\rho_{1,\mathfrak{K}^*}^{n+1} - \rho_{1,\mathfrak{K}^*}^n}{\delta t} + \operatorname{div}^{\mathfrak{K}^*}(J_{1,\mathfrak{D}}^{n+1}) = 0 & \forall \mathfrak{K}^* \in \mathfrak{M}^* \cup \partial\mathfrak{M}_N^* \\ \frac{\rho_{2,\mathfrak{K}}^{n+1} - \rho_{2,\mathfrak{K}}^n}{\delta t} + \operatorname{div}^{\mathfrak{K}}(J_{2,\mathfrak{D}}^{n+1}) = \operatorname{div}^{\mathfrak{K}}(\mathbf{V}_{\mathfrak{D}}^{n+1} J_{1,\mathfrak{D}}^{n+1}) - \mathbf{V}_{\mathfrak{K}}^{n+1} \operatorname{div}^{\mathfrak{K}}(J_{1,\mathfrak{D}}^{n+1}) + \mathbf{W}_{\mathfrak{K}}^{n+1} & \forall \mathfrak{K} \in \mathfrak{M} \\ \frac{\rho_{2,\mathfrak{K}^*}^{n+1} - \rho_{2,\mathfrak{K}^*}^n}{\delta t} + \operatorname{div}^{\mathfrak{K}^*}(J_{2,\mathfrak{D}}^{n+1}) = \operatorname{div}^{\mathfrak{K}^*}(\mathbf{V}_{\mathfrak{D}}^{n+1} J_{1,\mathfrak{D}}^{n+1}) - \mathbf{V}_{\mathfrak{K}^*}^{n+1} \operatorname{div}^{\mathfrak{K}^*}(J_{1,\mathfrak{D}}^{n+1}) + \mathbf{W}_{\mathfrak{K}^*}^{n+1} & \forall \mathfrak{K}^* \in \mathfrak{M}^* \cup \partial\mathfrak{M}_N^* \\ -\lambda^2 \operatorname{div}^{\mathfrak{K}}(\nabla^{\mathfrak{D}} \mathbf{V}_{\mathfrak{T}}^{n+1}) = C_{\mathfrak{T}} - \rho_{1,\mathfrak{K}}^{n+1} & \forall \mathfrak{K} \in \mathfrak{M} \\ -\lambda^2 \operatorname{div}^{\mathfrak{K}^*}(\nabla^{\mathfrak{D}} \mathbf{V}_{\mathfrak{T}}^{n+1}) = C_{\mathfrak{T}} - \rho_{1,\mathfrak{K}^*}^{n+1} & \forall \mathfrak{K}^* \in \mathfrak{M}^* \cup \partial\mathfrak{M}_N^* \end{array} \right. \quad (3.2)$$

coupled with Neumann boundary conditions:

$$J_{1,\mathfrak{D}}^{n+1} \cdot \mathbf{n}_{\sigma\mathfrak{K}} = J_{2,\mathfrak{D}}^{n+1} \cdot \mathbf{n}_{\sigma\mathfrak{K}} = (\nabla^{\mathfrak{D}} \mathbf{V}_{\mathfrak{K}}^{n+1}) \cdot \mathbf{n}_{\sigma\mathfrak{K}} = 0 \quad \forall \sigma \in \partial\mathfrak{M}_N \quad (3.3)$$

where $\rho_{i,\mathfrak{T}}^{n+1} = \rho_i(\mathbf{u}_{\mathfrak{T}}^{n+1})$, $i = 1, 2$, and where the current densities (2.2) are discretized by rewriting $u_2 \nabla V = \nabla(u_2 V) - V \nabla u_2$, so we have:

$$J_{i,\mathfrak{D}}^{n+1} = -L_{i1}^{\mathfrak{D},n} (\nabla^{\mathfrak{D}} u_{1,\mathfrak{T}}^{n+1} + \nabla^{\mathfrak{D}} (u_{2,\mathfrak{T}}^{n+1} \mathbf{V}_{\mathfrak{T}}^{n+1})) - \mathbf{V}_{\mathfrak{D}}^{n+1} \nabla^{\mathfrak{D}} u_{2,\mathfrak{T}}^{n+1} - L_{i2}^{\mathfrak{D},n} \nabla^{\mathfrak{D}} u_{2,\mathfrak{T}}^{n+1}, \quad \text{for } i = 1, 2. \quad (3.4)$$

3.3. DDFV scheme in entropic variables. As in the continuous setting, see Sec. 2.1, the key point of the analysis of the scheme (3.2)-(3.3) is to use another set of variables which allows to symmetrize the problem. Then, problem (3.2)-(3.3) is formally equivalent to looking for $\mathbf{w}_{\mathfrak{I}}^{[0,t^*]} = (\mathbf{w}^n)_{n \in \{0, \dots, N\}} \in (\mathbb{E}_{\mathbf{g}}^{\Gamma_D})^{N+1}$ and $\mathbf{V}_{\mathfrak{I}}^{[0,t^*]} = (\mathbf{V}^n)_{n \in \{0, \dots, N\}} \in (\mathbb{E}_h^{\Gamma_D})^{N+1}$, such that:

$$\left\{ \begin{array}{ll} \frac{b_{1,k}^{n+1} - b_{1,k}^n}{\delta t} + \operatorname{div}^k(I_{1,\mathfrak{D}}^{n+1}) = 0 & \forall k \in \mathfrak{M} \\ \frac{b_{1,k^*}^{n+1} - b_{1,k^*}^n}{\delta t} + \operatorname{div}^{k^*}(I_{1,\mathfrak{D}}^{n+1}) = 0 & \forall k^* \in \mathfrak{M}^* \cup \partial\mathfrak{M}_N^* \\ \frac{b_{2,k}^{n+1} - b_{2,k}^n}{\delta t} + \operatorname{div}^k(I_{2,\mathfrak{D}}^{n+1}) = -b_{1,k}^n \frac{V_k^{n+1} - V_k^n}{\delta t} + \bar{W}_k^{n+1} & \forall k \in \mathfrak{M} \\ \frac{b_{2,k^*}^{n+1} - b_{2,k^*}^n}{\delta t} + \operatorname{div}^{k^*}(I_{2,\mathfrak{D}}^{n+1}) = -b_{1,k^*}^n \frac{V_{k^*}^{n+1} - V_{k^*}^n}{\delta t} + \bar{W}_{k^*}^{n+1} & \forall k^* \in \mathfrak{M}^* \cup \partial\mathfrak{M}_N^* \\ -\lambda^2 \operatorname{div}^k(\nabla^{\mathfrak{D}} V_{\mathfrak{I}}^{n+1}) = C_{\mathfrak{I}} - b_{1,k}^{n+1} & \forall k \in \mathfrak{M} \\ -\lambda^2 \operatorname{div}^{k^*}(\nabla^{\mathfrak{D}} V_{\mathfrak{I}}^{n+1}) = C_{\mathfrak{I}} - b_{1,k^*}^{n+1} & \forall k^* \in \mathfrak{M}^* \cup \partial\mathfrak{M}_N^* \end{array} \right. \quad (3.5)$$

and:

$$I_{1,\mathfrak{D}}^{n+1} \cdot \vec{\mathbf{n}}_{\sigma_k} = I_{2,\mathfrak{D}}^{n+1} \cdot \vec{\mathbf{n}}_{\sigma_k} = (\nabla^{\mathfrak{D}} V_k^{n+1}) \cdot \vec{\mathbf{n}}_{\sigma_k} = 0 \quad \forall \sigma \in \partial\mathfrak{M}_N \quad (3.6)$$

where $b_{i,\mathfrak{I}}^{n+1} = b_i(\mathbf{w}_{\mathfrak{I}}^{n+1}, V_{\mathfrak{I}}^{n+1})$, $i = 1, 2$ and:

$$I_{i,\mathfrak{D}}^{n+1} = -D_{i1}^{\mathfrak{D},*} \nabla^{\mathfrak{D}} w_{1,\mathfrak{I}}^{n+1} - D_{i2}^{\mathfrak{D},*} \nabla^{\mathfrak{D}} w_{2,\mathfrak{I}}^{n+1}, \quad \text{for } i = 1, 2.$$

The coefficients of the matrix $D_{\mathfrak{D}}^* = (D_{ij}^{\mathfrak{D},*})$ for $i, j = 1, 2$ are defined in an explicit-implicit way as the coefficients of the matrix $D_{\mathfrak{D}}^* = {}^t P_{\mathfrak{D}}^{n+1} L_{\mathfrak{D}}^n P_{\mathfrak{D}}^{n+1}$, where $P_{\mathfrak{D}}^{n+1}$ is an approximation of the matrix P given by (2.7).

PROPOSITION 3.2. *We assume that $D_{\mathfrak{D}}^* = {}^t P_{\mathfrak{D}}^{n+1} L_{\mathfrak{D}}^n P_{\mathfrak{D}}^{n+1}$ holds and that $\mathbf{w}_{\mathfrak{I}}^{\mathfrak{I},[0,t^*]}$ and $\mathbf{u}_{\mathfrak{I}}^{\mathfrak{I},[0,t^*]}$ satisfy the following discrete counterpart of (2.4), i.e. for $n \in \{0, \dots, N\}$:*

$$\mathbf{w}_{1,\mathfrak{I}}^n := \mathbf{u}_{1,\mathfrak{I}}^n + \mathbf{u}_{2,\mathfrak{I}}^n V_{\mathfrak{I}}^n, \quad \mathbf{w}_{2,\mathfrak{I}}^n := \mathbf{u}_{2,\mathfrak{I}}^n. \quad (3.7)$$

Then, schemes (3.2)-(3.3) and (3.5)-(3.6) are equivalent.

Proof (sketch). We consider the first equation of (3.2). By definition, $b_i(\mathbf{w}_{\mathfrak{I}}^n, V_{\mathfrak{I}}^n) = \rho_i(\mathbf{u}_{\mathfrak{I}}^n) \forall n$, so that $\rho_{1,k}^{n+1} - \rho_{1,k}^n = b_{1,k}^{n+1} - b_{1,k}^n$.

Then, if we apply the change of variables (3.7) in (3.4), we get:

$$J_{1,\mathfrak{D}}^{n+1} = -L_{11}^{\mathfrak{D},n} \nabla^{\mathfrak{D}} w_{1,\mathfrak{I}}^{n+1} - (L_{12}^{\mathfrak{D},n} - L_{11}^{\mathfrak{D},n} V_{\mathfrak{D}}^{n+1}) \nabla^{\mathfrak{D}} w_{2,\mathfrak{I}}^{n+1}.$$

Since the definition of $D_{\mathfrak{D}}^*$ gives $D_{11}^{\mathfrak{D},*} = L_{11}^{\mathfrak{D},n}$ and $D_{12}^{\mathfrak{D},*} = L_{12}^{\mathfrak{D},n} - L_{11}^{\mathfrak{D},n} V_{\mathfrak{D}}^{n+1}$, we deduce that $\operatorname{div}^k(J_{1,\mathfrak{D}}^{n+1}) = \operatorname{div}^k(I_{1,\mathfrak{D}}^{n+1})$. To prove the equivalence of the other equations, we proceed similarly.

3.4. Discrete entropy dissipation. In this section, we state the discrete counterpart of the entropy inequality of Prop. 2.2. Let $\mathbf{g} = (g_1, g_2)$; by Hyp. 2.1, (g_1, g_2) are defined on all the domain Ω , with $g_2 < 0$ constant; let $\mathbf{g}_{\mathfrak{I}} = ((\mathbf{g}_k)_{k \in \mathfrak{M}}, (\mathbf{g}_{k^*})_{k^* \in \mathfrak{M}^* \cup \partial\mathfrak{M}_N^*})$, $h_{\mathfrak{I}} = ((h_k)_{k \in \mathfrak{M}}, (h_{k^*})_{k^* \in \mathfrak{M}^* \cup \partial\mathfrak{M}_N^*})$ with \mathbf{g}_k, h_k the mean-value of the datas \mathbf{g}, h on $k \in \mathfrak{M}$ (resp. on $k^* \in \mathfrak{M}^* \cup \partial\mathfrak{M}_N^*$).

For all $n \in \{0, \dots, N\}$, the discrete DDFV entropy functional is defined as:

$$S^n = \frac{1}{2} \sum_{\mathbf{k} \in \mathfrak{M}} m_{\mathbf{k}} \left(\rho_{\mathbf{k}}^n \cdot (\mathbf{u}_{\mathbf{k}}^n - \mathbf{g}_{\mathbf{k}}) - (\chi(\mathbf{u}_{\mathbf{k}}^n) - \chi(\mathbf{g}_{\mathbf{k}})) \right) \\ + \frac{1}{2} \sum_{\mathbf{k}^* \in \mathfrak{M}^* \cup \partial \mathfrak{M}^*} m_{\mathbf{k}^*} \left(\rho_{\mathbf{k}^*}^n \cdot (\mathbf{u}_{\mathbf{k}^*}^n - \mathbf{g}_{\mathbf{k}^*}) - (\chi(\mathbf{u}_{\mathbf{k}^*}^n) - \chi(\mathbf{g}_{\mathbf{k}^*})) \right) - \frac{1}{2} g_2 \|\nabla^{\mathfrak{D}}(\mathbf{V}_{\bar{x}}^{n+1} - h_{\bar{x}})\|_{2, \mathfrak{D}}^2.$$

PROPOSITION 3.3 (Discrete entropy dissipation). *Assuming Hyp. 2.1 and thermal equilibrium for the Dirichlet boundary conditions, i.e. $\nabla^{\mathfrak{D}} \bar{g}_1^{\bar{x}} = \nabla^{\mathfrak{D}} \bar{g}_2^{\bar{x}} = 0$, the discrete entropy satisfies $\forall n \geq 0$:*

$$\frac{S^{n+1} - S^n}{\delta t} = -\delta t \sum_{\mathfrak{D} \in \mathfrak{D}} \left(D_{11}^{\mathfrak{D}, n} |\nabla^{\mathfrak{D}} w_{1, \bar{x}}^{n+1}|^2 + D_{22}^{\mathfrak{D}, *} |\nabla^{\mathfrak{D}} w_{2, \bar{x}}^{n+1}|^2 \right) + \delta t \left[[\mathbf{W}_{\bar{x}}^{n+1}, (\mathbf{u}_{2, \bar{x}}^{n+1} - g_{2, \bar{x}})] \right]_{\bar{x}} \leq 0.$$

This proposition is crucial since it gives a discrete $L^2(0, t^*, H^1)$ estimate on w_1 and w_2 . Following [5, 11], this is a first step in order to obtain other *a priori* estimates on the solution, who would lead to prove existence results for the scheme and then, by showing the compactness of the sequence of approximate solutions, to the convergence study of the scheme.

4. Numerical simulations. For the numerical simulations, we consider the energy-transport model under *parabolic band approximation* and *Maxwell-Boltzmann* statistics (see [12, 5, 11]). The densities ρ_1 and ρ_2 depend non-linearly on \mathbf{u} :

$$\rho_1(\mathbf{u}) = \left(-\frac{1}{u_2} \right)^{\frac{3}{2}} \exp(u_1), \quad \rho_2(\mathbf{u}) = \frac{3}{2} \left(-\frac{1}{u_2} \right)^{\frac{5}{2}} \exp(u_1).$$

The matrix L also depends on \mathbf{u} (we recall $T = -1/u_2$) and it can be written as :

$$L = c_0 \rho_1 T^{1/2-\beta} \begin{pmatrix} 1 & (2-\beta)T \\ (2-\beta)T & (3-\beta)(2-\beta)T^2 \end{pmatrix}, \quad (4.1)$$

where c_0 and β are constants. The usual values are $c_0 = 1$, $\beta = 1/2$, for the Chen model, and $c_0 = 2/\sqrt{\pi}$, $\beta = 0$ for the Lyumkis model. The energy relaxation term W is:

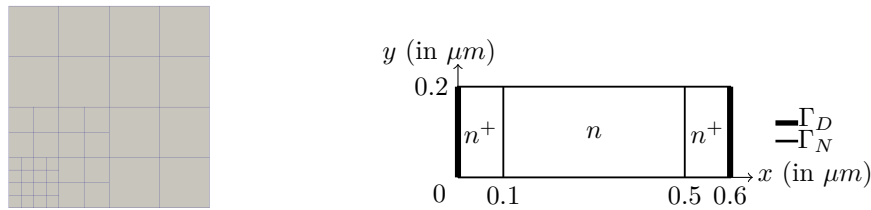
$$W = c_1 \rho_1 \frac{L^2}{\tau_0 \mu_0 U_T} T^{\beta-1/2} (1-T) \quad (4.2)$$

where $c_1 = 3/2$ for the Chen model, $c_1 = 2/\sqrt{\pi}$ for the Lyumkis model.

It is an ongoing work: we present here the first simulations obtained by expliciting in time the schemes (3.2)-(3.3) and (3.5)-(3.6). Section 4 is devoted to the simulation of a 2D-ballistic silicon diode, where we compare the results obtained by Chen and Lyumkis models.

For all numerical simulations that we present, we tested both (3.2)-(3.3) and (3.5)-(3.6), on a large class of general meshes. All the simulations gave equivalent results; we present here the results on a refinement (with 2560 cells) of the non-conformal locally refined mesh of Fig. 4.1, obtained with the first scheme (3.2)-(3.3). The physical data are taken from [10].

2D ballistic diode. We present the results for a 2-dimensional ballistic n^+mn^+ silicon diode, which is uniform in one space dimension; we resume the parameters for silicon in Tab. 4.1. We will compare the shape and the maximum values of our numerical results to the ones in [6, 10, 4].

Fig. 4.1: *Left*: non conformal square mesh. *Right*: physical geometry of the n^+nn^+ diode.

| Parameter | Value | Parameter | Value |
|--------------------------------------|--------------------------|-----------------------------------|-----------|
| q (elementary charge) | 1.6d-19 As | T_0 (ambient temperature) | 300 K |
| ϵ_s (permittivity constant) | 1.d-12 As $V^{-1}s^{-1}$ | U_T (thermal voltage at T_0) | 0.0259 V |
| μ_0 (low field mobility) | 1.5d3 $cm^2V^{-1}s^{-1}$ | τ_0 (energy relaxation time) | 0.4d-12 s |

Table 4.1: : Physical parameters for silicon.

The semiconductor domain, before scaling (see [10] for details), is $\Omega = (0, l_x) \times (0, l_y)$, where $l_x = 0.6\mu m$ and $l_y = 0.2\mu m$ and the length of the channel equals $0.4\mu m$. It is presented in Fig. 4.1.

For this test case, we set $C_m = 5.d17 \text{ cm}^{-3}$, $C_n = 2.d15 \text{ cm}^{-3}$, and the applied voltage $V_{app} = 1.5V$. The rescaled doping is defined as $C(x, y) = C_n/C_m$ in the n region, $C(x, y) = 1$ in the n^+ region, where the n region is $[\frac{\ell_0}{\ell_x}, 1 - \frac{\ell_0}{\ell_x}] \times [0, 1]$, with $\ell_0 = 1d-4m$. We initialize $\mathbf{u} = (u_1, u_2)$ and V with $\mathbf{u}_0(x, y) = (0, 1)$ and $V_0(x, y) = V_{app}/U_T$ if $x = 0$, $V_0(x, y) = 0$ otherwise.

Fig. 4.2-4.3 show the solution of the unstationary system at a fixed time step, i.e. the equilibrium, which is attained at different instants (according to the chosen mesh and model); in all cases, the equilibrium instant $t_{eq}^* \in [0.1, 0.5]$. The time step chosen for the explicit scheme is $\delta t = 0.5d - 7$.

We present in Fig. 4.2 the variations of the temperature in the diode, and in Fig. 4.3 the electron mean velocity, defined as $v^{el} = \|J_1\|_1 / (q\rho_1)$; in both cases, we compare the solution computed with the Chen and Lyumkis model, for which we have references in [6, 10, 4]. As expected, the computed quantities are uniform in one space direction and we can see the hot electron effect in the channel.

In Fig. 4.2, remark that the temperature is high in the n -channel and that its shape and its maximum depend on the model. For the Chen model, the maximum is attained at $T = 7.86K$, which corresponds (before scaling) to $T = 2358K$: the reference is $T_{ref} = 2330K$. For the Lyumkis model, the maximum is at $T = 12.9K$, which corresponds (before scaling) to $T = 3871K$: the reference is $T_{ref} = 3970K$.

In Fig. 4.3, we compare the values of the electron mean velocity. For the Chen model, the maximum is attained at $v^{el} = 23.2 \text{ cm/s}$, which corresponds (before scaling) to $v^{el} = 1.49 \cdot 10^7 \text{ cm/s}$: the reference is $v^{el} = 1.44 \cdot 10^7 \text{ cm/s}$. For the Lyumkis model, the maximum is at $v^{el} = 42.48 \text{ cm/s}$, which corresponds (before scaling) to $v^{el} = 2.75 \cdot 10^7 \text{ cm/s}$: the reference is $v^{el} = 2.92 \cdot 10^7 \text{ cm/s}$.

REFERENCES

- [1] B. ANDREIANOV, F. BOYER, AND F. HUBERT, *Discrete duality finite volume schemes for Leray-Lions type elliptic problems on general 2D-meshes*, Num. Meth. for PDEs, 23(1):145-195, 2007.
- [2] M. BESSEMOULIN-CHATARD, C. CHAINAIS-HILLAIRET AND H. MATHIS, *Numerical schemes for semiconductors energy-transport models*, to appear in FVCA IX, Springer Proceedings in Mathematics and Statistics.
- [3] C. CHAINAIS-HILLAIRET, *Discrete duality finite volume schemes for two dimensional drift-diffusion and energy-transport models*, International Journal for Numerical Methods in Fluids 59(3):239 - 257, 2009.

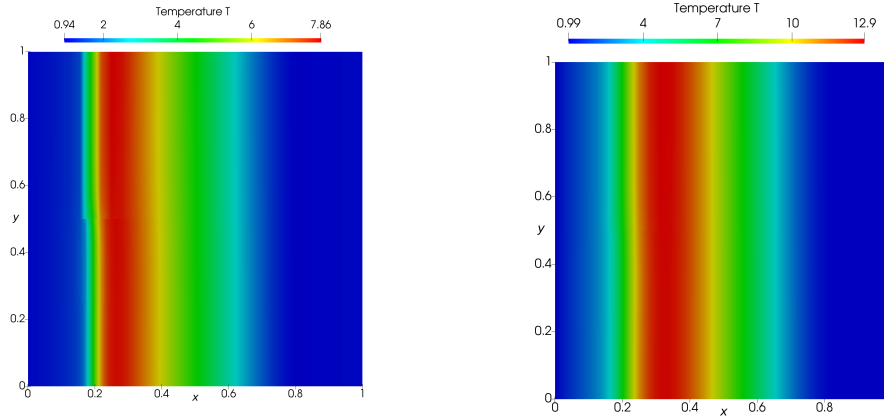


Fig. 4.2: Influence of parameters c_0 and β on the scaled temperature: Chen (*left*) and Lyumkis (*right*) model.

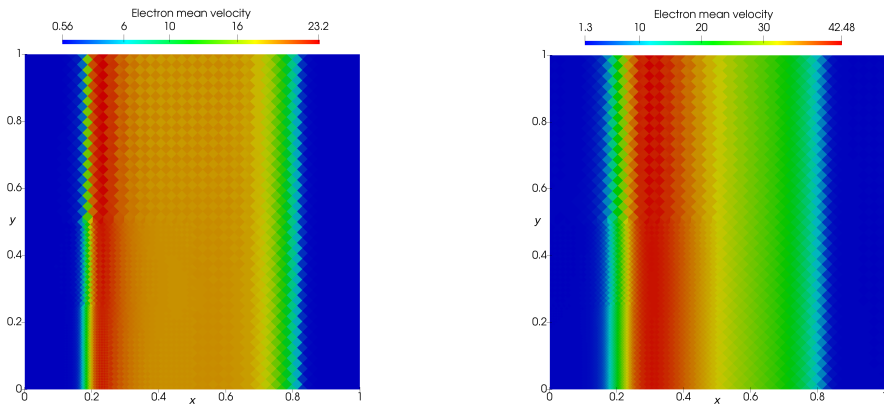


Fig. 4.3: Influence of parameters c_0 and β on the scaled electron mean velocity: Chen (*left*) and Lyumkis (*right*) model.

- [4] C. CHAINAIS-HILLAIRET AND Y. -J. PENG, *Finite Volume Scheme for Semiconductor Energy-transport Model*, pages 139-146. Birkäuser Basel, Basel, 2005.
- [5] P. DEGOND, S. GÉNEIEYS AND A. JUNGEL, *A system of parabolic equations in nonequilibrium thermodynamics including thermal and electrical effects*, J. Math. Pures Appl., 1997.
- [6] P. DEGOND, A. JUNGEL AND P. PIETRA, *Numerical discretization of energy-transport models for semiconductors with non-parabolic band structure*, SIAM Journal on Scientific Computing, 2000.
- [7] K. DOMELEVO AND P. OMNES, *A finite volume method for the Laplace equation on almost arbitrary two-dimensional grids*, M2AN Math. Model. Numer. Anal., 39(6):1203-1249, 2005.
- [8] M. FOURNIÉ, *Numerical discretization of energy-transport model for semiconductors using high-order compact schemes*, Appl. Math. Lett., 15(6):721-726, 2002.
- [9] F. HERMELINE, *A finite volume method for the approximation of diffusion operators on distorted meshes*, J. Comput. Phys., 160(2):481-499, 2000.
- [10] S. HOLST, A. JUNGEL AND P. PIETRA, *A mixed Finite-Element Discretization of the Energy- Transport model for semiconductors*, SIAM Journal on Scientific Computing, 2003.
- [11] A. JUNGEL, *Quasi-hydrodynamic semiconductor equations* Birkhäuser, 2001.
- [12] A. JUNGEL, *Transport equations for semiconductors*, Lecture Notes in Physics, 773, 2009.
- [13] S. KRELL, *Schémas Volumes Finis en mécanique des fluides complexes*, PhD thesis, Univ. de Provence, 2010.